Earth Syst Environ (2017) 1:3
DOI 10.1007/s41748-017-0003-0

ORIGINAL ARTICLE

Impact of Different Cumulus Parameterization Schemes in SAUDI-KAU AGCM

Muhammad Azhar Ehsan[1] · **Mansour Almazroui**[1] · **Ahmed Yousef**[1]

Received: 27 January 2017 / Accepted: 7 April 2017 / Published online: 26 April 2017

Abstract
Background In global climate models (GCMs), the convection is parameterized, since the typical scale of this process is smaller than the model resolution.
Purpose This study examines the impact of two different cumulus parameterization schemes on the simulated climate using single-column model (SCM) as well as in an atmospheric global climate model (AGCM).
Methods The two schemes used are: the Simplified Arakawa–Schubert (SAS) scheme; and the Emanuel scheme coupled with a probability distribution function-based cloud parameterization scheme (EMAN).
Results The humidity, temperature, cloud fraction, and precipitation simulations are improved in EMAN as compared to that of SAS in SCM. Climatological simulations (1981-2014) conducted using an AGCM at a moderate resolution (T106L44: 1.125° × 1.125°) indicated that the use of the EMAN improved the results. The precipitation over the tropical belt also showed improvements in terms of the distributions, biases, and association with observation. These improvements are attributable to a better vertical structure of temperature, especially in the tropics, due to the more realistic estimation of the temperature and moisture fields by the EMAN. The error estimated in outgoing long-wave radiation for EMAN is lower than that of the SAS. The vertical structure of specific humidity and temperature shows less error in EMAN as compared to SAS.
Conclusion Results using the SCM and AGCM reveal the benefits of using the EMAN in comparison to the SAS which includes better simulation of the relative humidity, temperature, and precipitation fields.

Keywords SAUDI-KAU · AGCM · SAS · Emanuel · PDF cloud scheme · OLR

1 Introduction

Atmospheric global climate models (AGCMs) are valuable tools to explore the atmosphere–ocean and land–atmosphere interactions and to understand better past climate and as well as future climate scenarios. In AGCMs, convection is parameterized, because the characteristic scale of this atmospheric process is smaller than the typical global model resolution. AGCMs simulations are strongly influenced by their cumulus convection parameterization schemes (CPSs) and, in particular, precipitation simulated by AGCMs is strongly dependent on the CPSs. Thus, appropriate CPSs are required in AGCMs for realistic climate simulations. CPSs in AGCMs have been the subject of intensive research for the last four decades (e.g., Arakawa 2004 and references there in). Based on different physical assumptions and having their own strengths and weaknesses, a great selection of CPSs is available (e.g., Kuo 1965; Arakawa and Schubert 1974; Betts and Miller 1986; Tiedtke 1989; Gregory and Rowntree 1990; Emanuel 1991; Kain and Fritsch 1993; Zhang and McFarlane 1995), applied and used in different AGCMs and has revealed their explicit influences on the climate simulated by the host model (Lee et al. 2003; Zhang and Mu 2005; Kang and Hong 2008; Yang et al. 2014; Yousef et al. 2017).

✉ Muhammad Azhar Ehsan
azhar.ehsan82@gmail.com

[1] Department of Meteorology, Center of Excellence for Climate Change Research (CECCR), King Abdulaziz University, P.O. Box: 80208, Jeddah 21589, Saudi Arabia

Several previous studies highlighted the importance of CPSs and showed the strength of selected scheme in simulating both regional and global climatic features (Lee et al. 2003; Tost et al. 2006; Pezzi et al. 2008). Lee et al. (2003) compared different CPSs in idealized (aqua-planet) as well as realistic (AGCM) simulations. They found large differences in simulating the tropical intraseasonal oscillation (ISO), mean thermodynamic state and the Intertropical Convergence Zone (ITCZ) among different CPSs. Tost et al. (2006) compared different CPSs in ECHAM5 and found that all schemes gave robust results with stable and realistic meteorology over a selected 6-year period. Similarly, precipitation distribution and intensity are significantly improved over the tropics in the revised schemes described in Zhang and Mu (2005), Yang et al. (2014) and Yousef et al. (2017). These revised schemes also showed potential changes on the mean and variability of Arabian Peninsula's precipitation as compared to original CPSs (Zhang and Mu 2005; Yang et al. 2014; Yousef et al. 2017). This further explains that apart from the global scale, CPSs also greatly impact regional climate. In this study, two different CPSs are implemented in an AGCM, in order to highlight their strength and weakness and account for feedbacks on the simulated meteorology.

The paper is organized as follows: Sect. 2 presents a brief introduction to the model and convection parameterizations used in this study. The single-column model (SCM) experiment setup, data, methodology and results are described in Sect. 3. Section 4 discusses the results, which have been obtained from the full AGCM using two different CPSs. Section 5 contains relative merits of one CPS over the other and Sect. 6 contains a summary and conclusions.

2 The Model Description and CPSs Used

2.1 The Model Description

The model used in this study is the SAUDI King Abdulaziz University Atmospheric Global Climate Model (SAUDI-KAU AGCM: Ehsan et al. 2017). The SAUDI-KAU AGCM is actually based on the Seoul National University global spectral climate model (SNU-GCM; Lee et al. 2001; 2003), which was originally based on the Center for Climate System Research (CCSR)/National Institute for Environmental Studies (NIES) AGCM (Numaguti et al. 1995). Except for the newly implemented Emanuel scheme, the dynamics and physics options in the current study are the same as described in Lee et al. (2001) and later studies. These include shallow convection (Tiedtke 1984), non-local PBL/vertical diffusion scheme described in (Holtslag and Boville 1993), and a land surface model (Bonan 1996) of Community Climate Model (CCM3) which is obtained from the National Center for Atmospheric Research (NCAR). The deep cumulus convection scheme is a simplified version of the Arakawa–Schubert scheme (SAS: Numaguti et al. 1995). The large-scale condensation consists of a prognostic microphysics parameterization of total cloud liquid water (Le Treut and Li 1991) with a diagnostic cloud fraction parameterization. Radiation is parameterized by the 2-stream k-distribution scheme (Nakajima et al. 1995). The individual CPSs are well documented in detail in the literature (Lee et al. 2001, 2003; Emanuel and Zivkovic-Rothman 1999; Bony and Emanuel 2001), and here we briefly review the two schemes used for this study.

2.2 The SAS CPS

SAS assumes a spectrum of clouds of different sizes at different stages of their life cycle. The cloud model used in the SAS is of the ''entraining plume'' type, in which air rises through the cloud base level, and mixes with laterally entrained environmental air as it moves upward. Detrainment is arbitrarily allowed only at the cloud top. The cumulus mass flux at the cloud base M_B relaxes the cloud work function A toward neutral stability with a specified adjustment time scale:

$$M_B = M_o \frac{A}{A - A'} \frac{\Delta t}{\tau}$$

where Δt is the AGCM time step, and τ is the adjustment time scale. A' is a perturbed cloud work function, computed in response to a small trial M_o mass flux. Cloud work function (Eq. 1 in Lee et al. 2003) is the mass flux-weighted buoyancy integral. If entrainment is zero, this simply represents Convective Available Potential Energy (CAPE). Further, the adjustment time scale τ in this study is currently set to 4800 s and Δt is 300 s. The SAS and its variants have been used in many previous studies (Lee et al. 2003; Yang et al. 2014; Yousef et al. 2017).

2.3 The Emanuel (EMAN) CPS

The second convection scheme used in this study was originally developed by Emanuel (1991) and subsequently modified and optimized by Emanuel and Zivkovic-Rothman (1999). The cloud model used in the Emanuel is based on "buoyancy sorting" concept, which is based on the episodic mixing model of Raymond and Blyth (1986). It assumes that mixing in clouds is highly episodic and inhomogeneous, rather than continuous as in the entraining plume model. Air that is mixed into a cloud from the environment is assumed to form a spectrum of mixtures of differing mixing fraction, which then ascend or descend to their respective levels of neutral buoyancy. The Emanuel CPS is meant to represent the effects of all moist convection, including shallow, non-precipitating cumulus.

As depicted in Emanuel and Živković-Rothman (1999), the fraction of the total cloud base mass flux, M_B, which mixes with its environment at any level is here set proportional to the rate of change with altitude of the undiluted buoyancy:

$$\frac{\delta M}{M_B} = \frac{|\delta B| + \Lambda \delta p}{\sum_{i=1}^{N} (|\delta B| + \Lambda \delta p)}$$

where δM is the rate of mixing of undiluted cloudy air, δB and δp are a change in undilute buoyancy (B) and pressure (p) over a pressure interval, respectively; Λ is a mixing parameter, and N is the number of vertical model levels. The mixing rate can result in either entrainment or detrainment, depending on the buoyancy of the resulting mixtures. The absolute value of buoyancy reveals that increasing buoyancy with height can be expected to enhance entrainment while decreasing buoyancy enhances detrainment, or it increases the rate of mixing. The mass flux through the cloud base M_B is determined using sub-cloud-layer quasi-equilibrium hypothesis as described in Raymond (1995), which states that the convective mass fluxes will adjust so that air within the subcloud-layer remains neutrally buoyant with respect to upward displacements to just above the top of the subcloud layer. The idea is based on the fact that the time scale for surface fluxes and radiative cooling to destabilize the subcloud layer is relatively short.

The Emanuel scheme is then coupled with the cloud parameterization described in Bony and Emanuel (2001), following the idea that the convection scheme predicts the local concentration of condensed water (the in-cloud water content) produced at the sub-grid scale, and that a statistical cloud scheme predicts how this condensed water is spatially distributed within the domain. This cloud scheme uses a generalized lognormal probability distribution function (PDF) of the total water content whose variance and skewness coefficients are diagnosed from the amount of condensed water produced at the sub-grid scale by cumulus convection (Bony and Emanuel 2001). The cloud fraction and the domain-averaged amount of condensate are obtained by integrating the PDF over the saturated domain. Recently the Emanuel scheme (EMAN) has been implemented and tested in SAUDI-KAU AGCM framework (Ehsan et al. 2017), and showed quite satisfactory results in simulating the mean and variability features over different Northern Hemisphere summer monsoon regions.

3 Single-Column Model Comparison

3.1 Simulation Setup and Data

An SCM is used to compare the two CPSs (EMAN and SAS). The SCM framework is a basic method for investigating and developing CPSs (Randall et al. 1996). Although the SCM is inadequate for understanding all of the impacts of CPSs on model simulation, it does characterize the performance of the CPSs in different convective situations. Here, the SCM is used in two experiments. In the first experiment, the SAS is used, and in the second experiment, the SCM uses the newly implemented EMAN scheme using data from the Tropical Ocean and Atmosphere Coupled Ocean Atmosphere Response Experiment (TOGA-COARE, Webster and Lukas 1992). The TOGA-COARE is a special observation program for tropical convection, and the data represent an average over the TOGA-COARE intensive flux array, a region of about 400 by 250 km with lat./lon. ranges of 2°S–4°S and 155°E–158°E. The initial conditions and forcing data are obtained from the TOGA-COARE and the Global Energy and Water Cycle Experiment (GEWEX) Cloud System Study (GCSS). The SCM experimentation setup described here is similar to the one described in Yousef et al. (2017).

3.2 Results and Discussion

In moist convective processes, moisture fields like relative humidity are the most sensitive variables (Emanuel 1991). The performance of the coupled cloud-convection scheme is, therefore, predominantly based on comparison of the observed and predicted evolutions of relative humidity (RH) during the TOGA-COARE experiment. Vertical RH profiles simulated by SAS and EMAN are compared with observation during two distinct periods of operation of the TOGA-COARE. Those periods are: period A (29 November–10 December 1992), which shows slowly increasing precipitation, and period B (9 January–21 January 1993) which shows active, suppressed and transition states of convection. Without any major tweaking of the EMAN in the SCM, there are improvements in the vertical profile of humidity at both lower and upper levels (Fig. 1). The improvement in the humidity profile is more pronounced during period A (Fig. 1a) than during period B (Fig. 1b). Owing to the global enthalpy constraint, a good prediction of the humidity profile almost guarantees a good prediction of the temperature profile (Emanuel and Zivkovic-Rothman 1999). The temperature profiles of the SCM simulations using SAS and EMAN are shown in Fig. 2. As compared to the relative humidity, the temperature profile is simulated well by the two CPSs for both periods.

The vertical profile of the mean fraction of cloud amount predicted by the two CPSs (SAS and EMAN) during the two periods of operation of TOGA-COARE is displayed in Fig. 3. Period A shows the suppressed period of the convection, and so the associated cloud fraction is also small, owing to the large saturation deficit of the

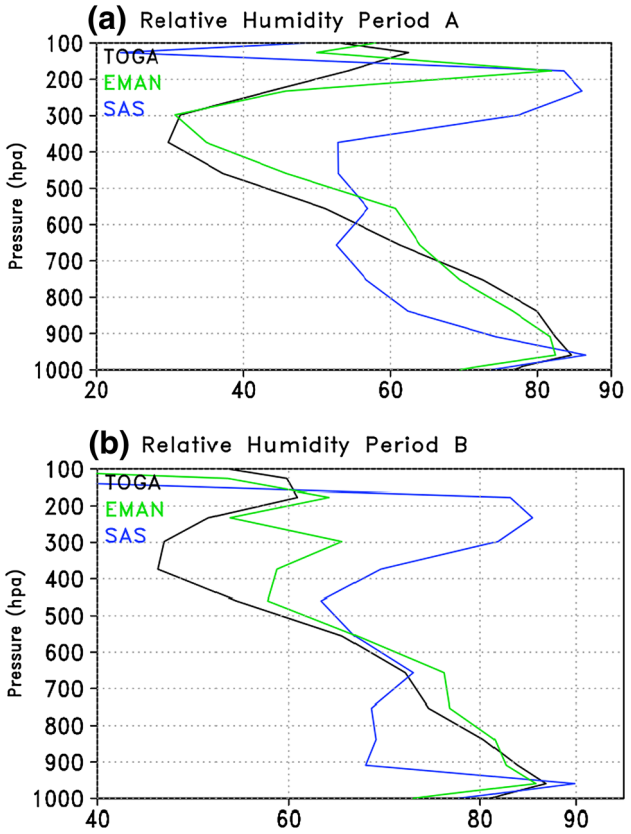

Fig. 1 The vertical profile of the relative humidity as simulated by the SAS and EMAN schemes for: **a** period A (29 November–10 December 1992) and **b** period B (9 January–21 January 1993) of TOGA-COARE IFA data. Unit of relative humidity is (%)

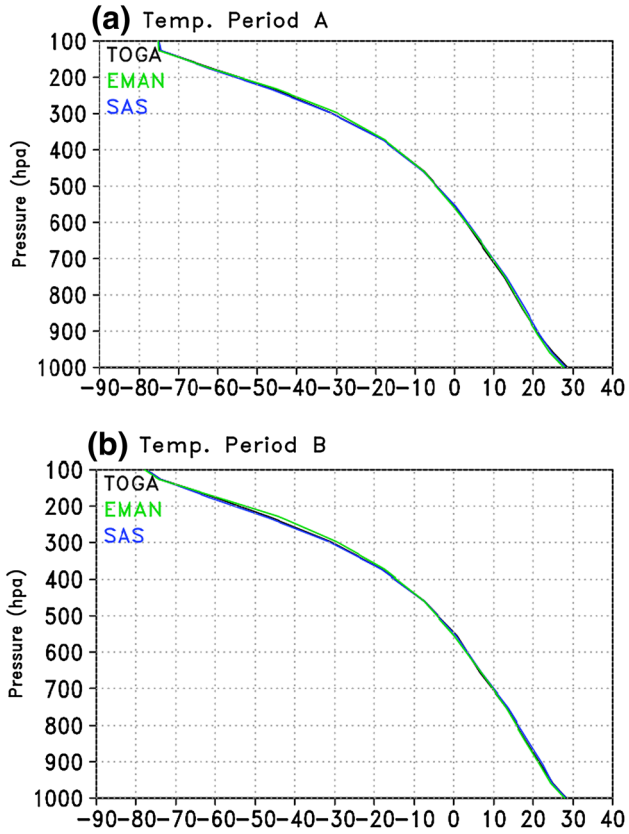

Fig. 2 Same as Fig. 1 but for temperature field. Unit of temperature is (°C)

environment (Fig. 3a). The SAS simulation exhibits more widespread cloudiness in the lowest level (between 1000–900 hPa) of the atmosphere than the other simulations. Indeed, extensive low-level clouds were not commonly observed during TOGA-COARE (Bony and Emanuel 2001). SAS shows quite high amount of cloudiness at these lower levels, which is not the case in EMAN (Fig. 3a, b). This shows the flimsier convective activity simulated by the SAS compared to the EMAN: the SAS produces less vertical transport due to convective mass flux, such that moisture produced at the surface resulting from latent heat flux largely remains in the lower atmosphere (within 100 hPa). Cloud fraction increases significantly with height above the 600 hPa (4–5 km, Fig. 3a). This is due to (1) the large amount of condensate produced by cumulus convection and, to a lesser extent, by large-scale condensation; and (2) to the smaller saturation deficit of the environment. Maxima are found around 200 hPa (12–13 km), where the detrainment is highest and it significantly moistens the environment (Fig. 3), and between 100–200 hPa. This average vertical distribution of the cloud cover results from the presence of different cloud types within the domain. To explain it further, we prepared the time series of the cloud fraction, which is shown in Fig. 4. The SAS tends to overestimate the cloud fraction during both periods. For instance, there is no activity during 13–14 January 1993 in reality. During these days, the EMAN shows almost zero cloudiness while SAS shows a cloud fraction of about 0.5.

Figure 5 shows a comparison of the observed and simulated precipitation from the SAS and EMAN during the periods A and B, respectively. The SAS (blue) and EMAN (green) are quite good in simulating precipitation during the two periods (Fig. 5a, b). For instance, during the period A, both CPSs simulate precipitation relatively well and the correlation coefficient (CC) of the SAS and EMAN with observations is 0.48 and 0.65, respectively, which shows that the EMAN performed better than the SAS. During the period B, both SAS and EMAN performed equally well with a CC of 0.74 and 0.79, respectively. In the next section, the impact of the two CPSs on the simulated climate is studied using the SAUDI-KAU AGCM on global scale.

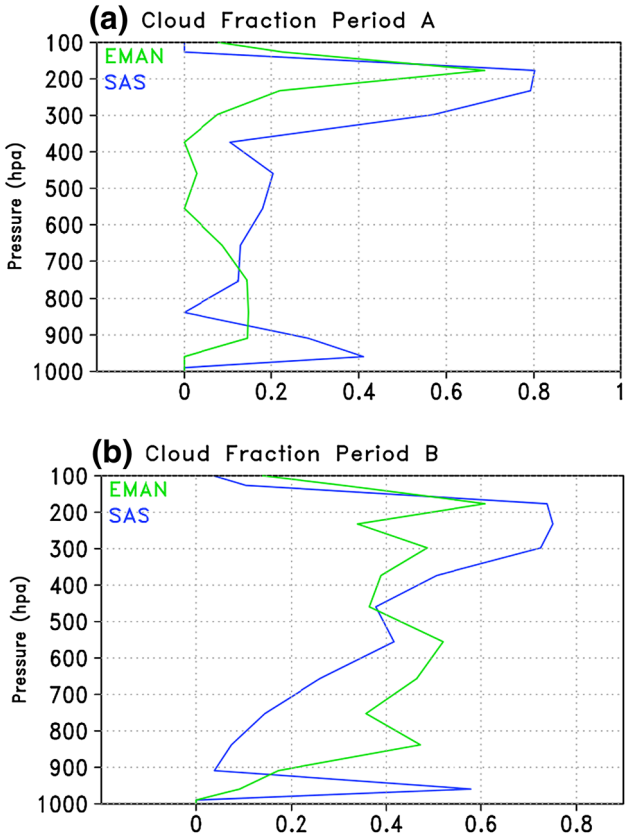

Fig. 3 Same as Fig. 1 but for cloud fraction. Cloud fraction is unit less

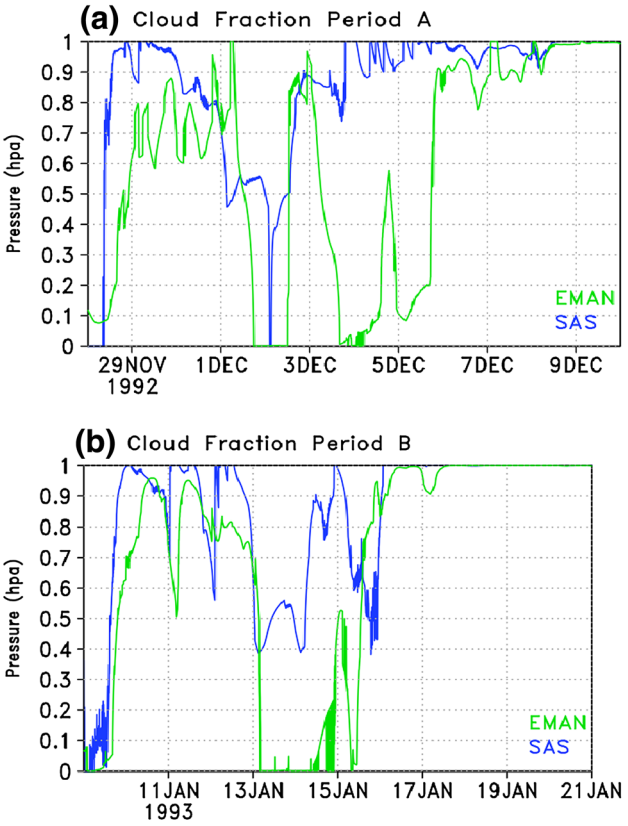

Fig. 4 Time series for the cloud fraction simulated by the SAS and EMAN schemes: **a** for the period A and **b** for the period B. Cloud fraction is unit less

4 Full Model (SAUDI-KAU AGCM) Comparison

4.1 Simulation Setup and Data

Two simulations were performed using SAUDI-KAU AGCM with SAS and EMAN. The model resolution used was T106L44 (triangular truncation at wave number T106 in the horizontal and 44 terrain-following sigma layers in the vertical), which is equivalent to $1.125° \times 1.125°$ grid resolution. The monthly varying sea surface temperature (SST) data are obtained from Hadley Centre SST dataset, HadISST1.1, and were used for the model simulations spanning 35 years, 1980–2014 (Rayner et al. 2003). The initial atmospheric data obtained from the NCEP Reanalysis-II (Kanamitsu et al. 2002) are used to initialize the AGCM. The integrations, started from the initial conditions at 00UTC of 01 January 1980, continued for the entire 35 years. For the data analysis, the first 6 months of all simulations were ignored (i.e., taken to be model spin-up time). The analysis is performed for the annual as well as two seasons (Dec-Mar: DJFM) and (Jun-Sep: JJAS) to make our comparison robust.

The observed precipitation data are obtained from Global Precipitation Climatology Project (GPCP) version 2.2 (Adler et al. 2003). Outgoing longwave radiation (OLR) data at the top of the atmosphere for the annual and seasonal mean were obtained from the Modern-Era Retrospective Analysis for Research and Application (MERRA; Rienecker et al. 2011). MERRA is a NASA reanalysis for the satellite era using a new version of the Goddard Earth Observing System Data Assimilation System Version 5 (GEOS-5). The specific humidity and temperature for the period 1981–2014 are obtained from the European Centre for Medium-Range Weather Forecasts (ECMWF) ERA-Interim reanalysis dataset (Dee et al. 2011). All these datasets are at different resolutions and were converted to a common $1° \times 1°$ grid resolution using bilinear interpolation. The observation-based total precipitation (TP: 3B42) and convective precipitation (CP: 3A12) estimates are also used here from Version 7 of the Tropical Rainfall Measuring Mission (TRMM) Multi-Satellite Precipitation Analysis, hereafter referred to as TRMM (Huffman et al. 2007) for the period 1998–2014. The TRMM datasets are used to compare the performance of two CPSs in simulating precipitation over the tropics.

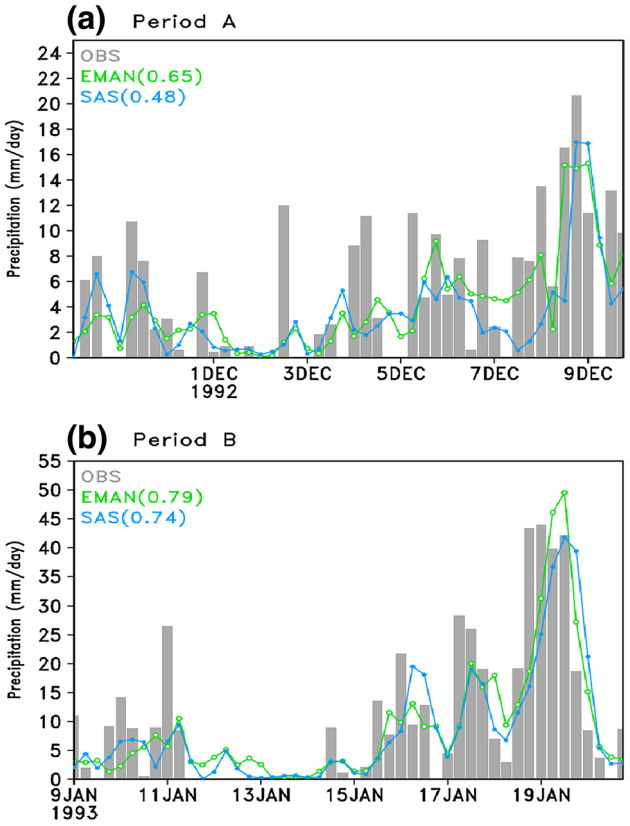

Fig. 5 Time series for the precipitation obtained from the TOGA-COARE data (*bars*), and simulated by SAS (*blue*) and EMAN (*green*) convection schemes: **a** for the first period A and **b** for the second period B. Unit of precipitation is mm/day. *Number within brackets* shows correlation coefficient between simulated and observed precipitation

4.2 Results and Discussion

Figure 6 shows annual mean precipitation of the GPCP and SAUDI-KAU AGCM simulations with two different CPSs for the period 1981–2014. Both simulations are able to reasonably capture prominent band-like structures in observation, such as the ITCZ and the south Pacific convergence zone (SPCZ). Both EMAN and SAS produce excessive precipitation over the Indian monsoon region compared to observation. EMAN shows further wet bias over the northwest Pacific and SPCZ regions. The mean annual biases estimated by the EMAN and SAS convection schemes are 0.39 and 0.43 mm/day, respectively, over the global domain. This indicates that simulated precipitation is overestimated either by EMAN or SAS as compared to the observation. The spatial correlation coefficient (SCC) is also estimated. SCC shows that two CPSs are quite comparable in mimicking the observation (Fig. 6b, c).

The seasonal mean JJAS precipitation over the global domain obtained from GPCP and the two CPSs is shown in Fig. 7. Both simulations are able to capture the general pattern of the JJAS precipitation over the globe as shown in the SCC. However, we can see that both CPSs overestimated the JJAS precipitation over the Indian and northwest Pacific regions. The EMAN scheme (Fig. 7b) shows excessive precipitation over these regions as compared to the SAS scheme (Fig. 7c). Over the African Monsoon region, EMAN shows a dry bias as compared to SAS. The overall bias and SCC estimated by the two CPSs are quite close to each other (Fig. 7b, c). Wang et al. (2005) and Wu et al. (2006) both show that the observed relationship between sea surface temperature and precipitation over the northwest Pacific region is poorly captured in AGCM simulations. Stan et al. (2010) showed that excessive precipitation over the west Pacific during boreal summer in the Community Atmosphere Model (CAM) is reduced (Khairoutdinov and Randall 2001) when the model is coupled to an ocean model. Consistent with Stan et al. (2010)'s results, the wet bias over the northwest Pacific and SPCZ regions is significantly reduced in our preliminary results from a coupled SAUDI-KAU model (not shown), confirming previous results that the bias partly comes from the lack of air-sea coupling (Kim and Kang 2011). The seasonal mean DJFM precipitation over the global domain obtained from GPCP and two CPSs is shown in Fig. 8. Again both simulations are able to capture the general pattern of the DJFM precipitation over the globe, with prominent regional differences. The double ITCZ, which is quite prominent in the SAS (Fig. 8c), is not produced by the EMAN (Fig. 8b). On the other hand, the EMAN shows quite high precipitation over the SPCZ and over the Indian Ocean.

The zonal mean values of simulated annual, JJAS and DJFM precipitations for the 34 years are shown in Fig. 9. Figure 9a indicates that the mean GPCP precipitation (black curve) from the annual mean has one maximum just north of the equator. Figure 9a clearly reveals that the simulations using the EMAN (red) are quite close to the observation curve. The SAS (green) shows a higher value to the north of the equator, which is about 2 mm/day more than observed. Outside the tropical regions, the two CPSs show quite comparable results. Figure 9b shows the zonal mean of JJAS precipitation. The two CPSs generally follow the observed zonal mean precipitation, with a slight overestimation. Figure 9c depicts the zonal mean distribution of DJFM precipitation obtained from observation and the two CPSs. In this season, the observation shows one peak just south of equator. This peak is also simulated by the two CPSs with slight overestimated precipitation (Fig. 9c). However, the SAS shows a much deeper peak in northern side of the equator, which is more than 2 mm/day than the observed one. Also it shows values higher than the observed peak just south of the equator. This "double

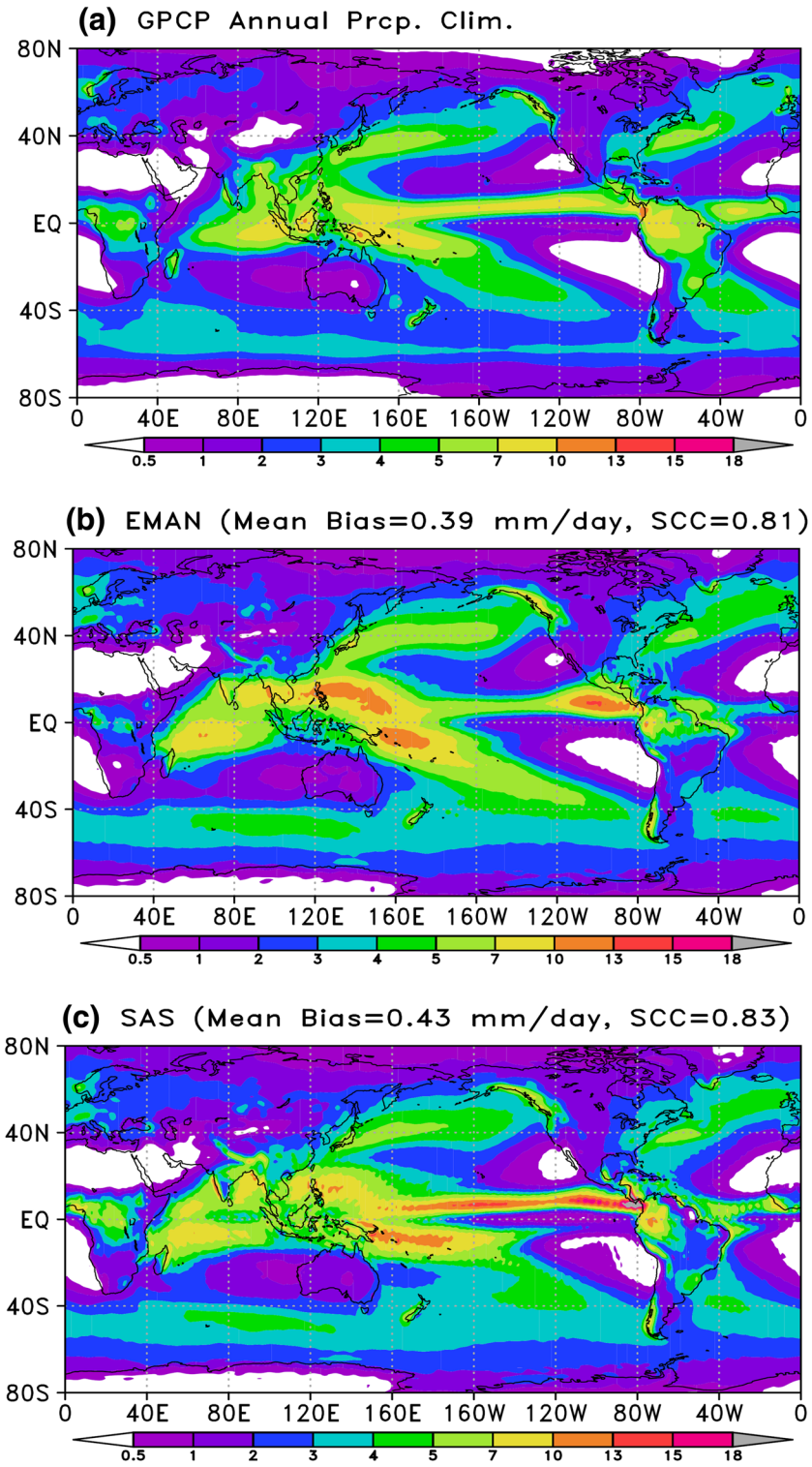

Fig. 6 Annual mean precipitation averaged over the period 1981–2014: **a** GPCP, **b** EMAN, and **c** SAS. Unit is mm/day. Mean bias (model—obs) and spatial correlation coefficient (SCC) are also shown for EMAN and SAS panels

ITCZ" is an intrinsic problem of the SAS in simulating the DJFM precipitation distribution right as compared to the observation, consistent with previous studies (e.g., Lee et al. 2003).

Statistics are calculated for the convective precipitation (CP) contribution of the model simulations compared with the CP product obtained from TRMM and shown in Table 1, for annual, JJAS and DJFM. It is apparent that the

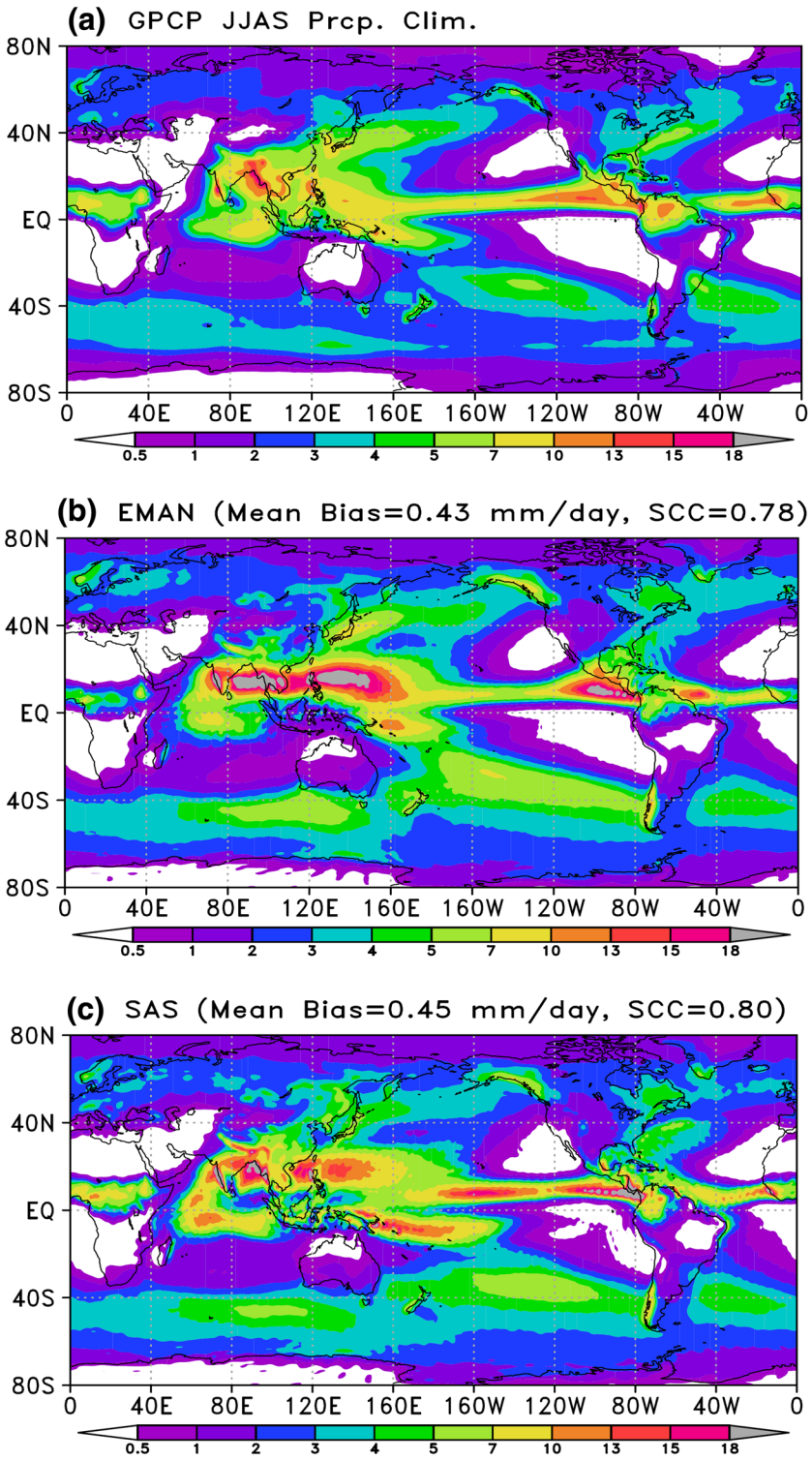

Fig. 7 Same as Fig. 6 but for JJAS season

SAS substantially overestimated the convective precipitation in the tropical region (0–360, 30°S–30°N), for annual as well as for two seasons. This overestimation (more than about 58%) also results in very high positive bias. On the other hand, EMAN shows mean CP quite close to the observed value (slightly underestimated) with a percentage bias not more than 10%. Nonetheless, the two CPSs show the SCC values quite comparable to each other (Table 1). The reason for this overestimation (underestimation) of the two CPSs (SAS and EMAN) compared to the TRMM data can be determined from the convective and stratiform components of precipitation, which is depicted in Table 1.

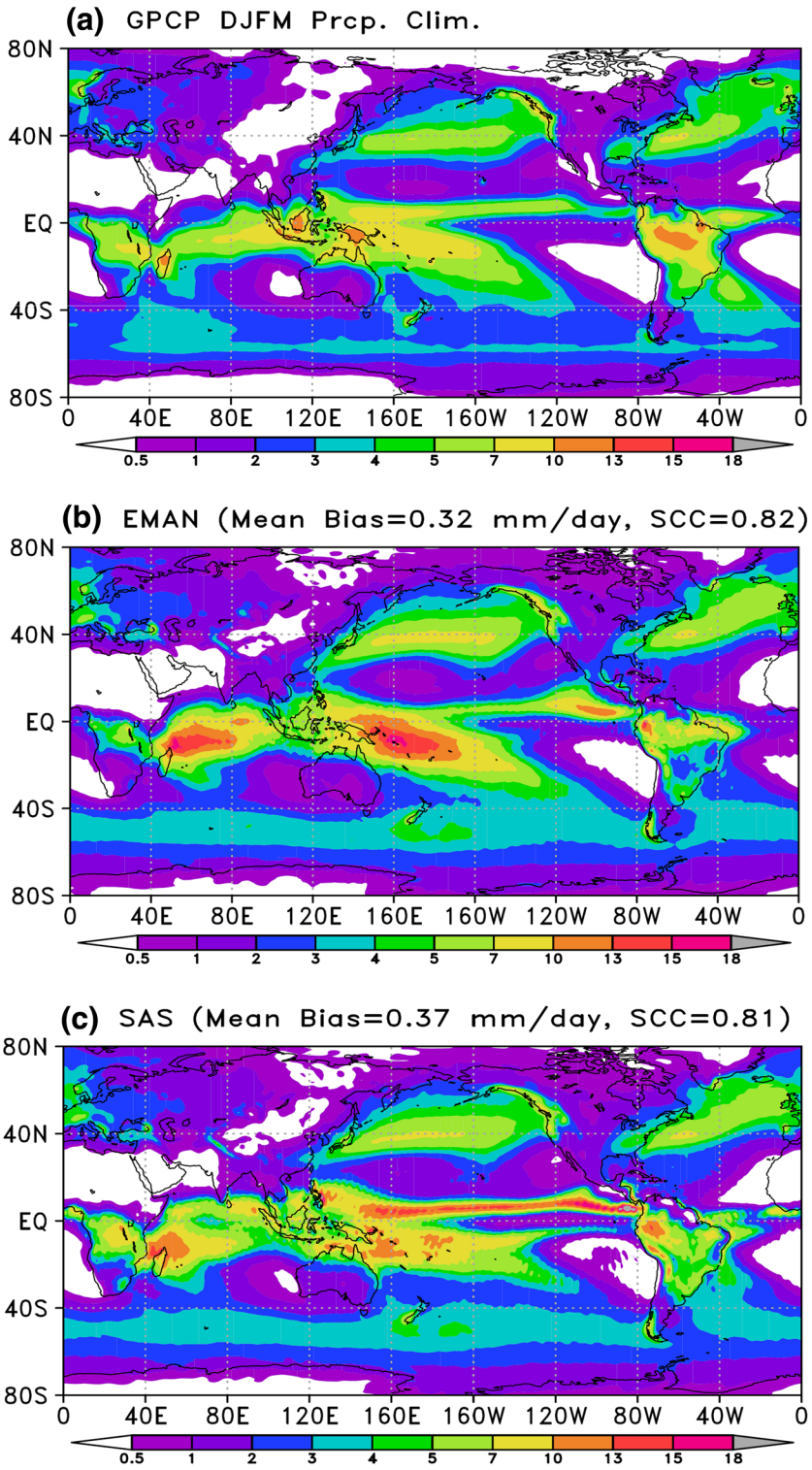

Fig. 8 Same as Fig. 6 but for DJFM season

In contrast to the TRMM data with a convective (stratifrom) fraction of about 40% (60%) in the tropics, the simulated precipitation fractions vary in EMAN and SAS from 42% (58%) to 70% (30%), respectively (see Table 1). In an inter-comparison study by Tost et al. (2006), it has been shown that models usually simulate the high convective contribution to the total precipitation (by some about 75%). The high values of the convective fraction in SAS scheme seem unrealistic, which could be due to the fact that the SAS scheme is sensitive to the convective instability (CAPE) and, therefore, the convective precipitation is generated too frequently, as soon as the CAPE is

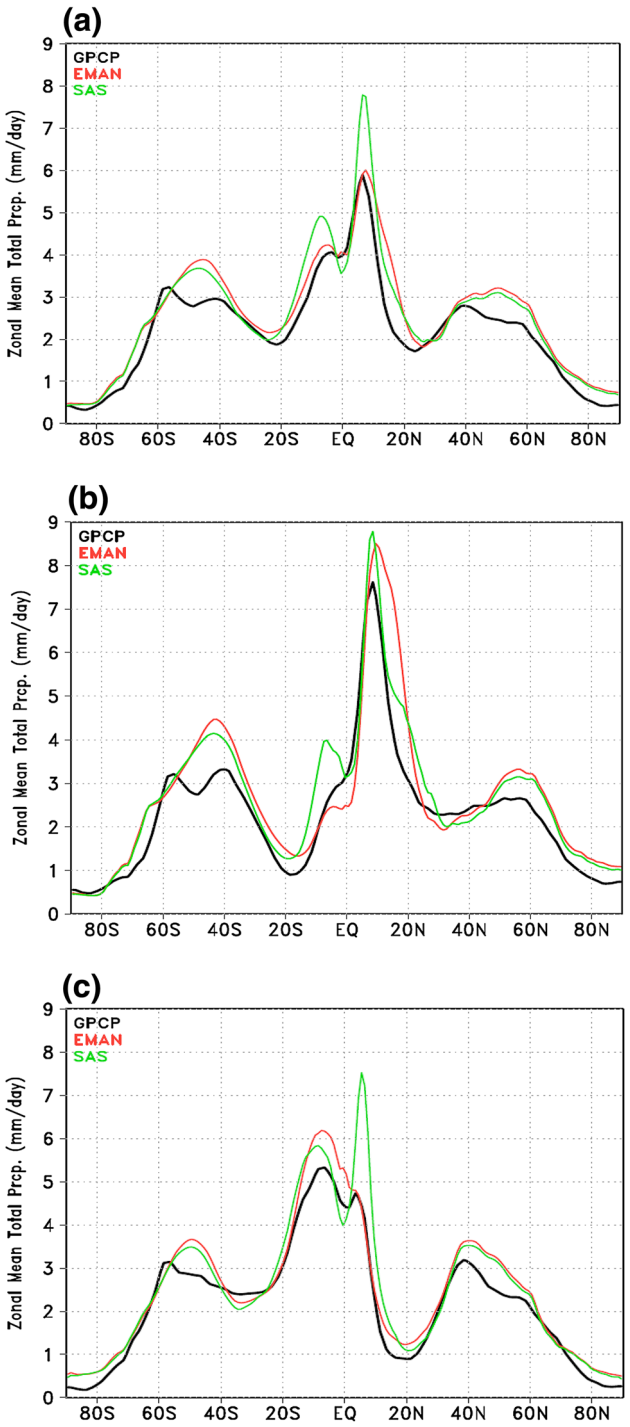

Fig. 9 Zonal mean: **a** annual, **b** JJAS, and **c** DJFM precipitation averaged over the period 1981–2014. Unit is mm/day

positive. However, the EMAN scheme not only depends on the CAPE but also this scheme is sensitive to the supply of the moisture (e.g., Emanuel and Zivkovic-Rothman 1999; Bony and Emanuel 2001). Further, it must be noted that the TRMM retrieval algorithm for the distinction of convective and stratiform of precipitation may not represent the reality perfectly, yet it provides useful information for comparing CPSs simulated convective precipitation.

Low (high) outgoing longwave radiation (OLR) values are indicative of enhanced (suppressed) convection and hence more (less) cloud coverage. The low OLR values (140–200 Wm^{-2}) shown in MERRA (Figs. 10a, 11a, 12a) match well with the local precipitation maximum in annual and seasonal mean (JJAS and DJFM). The annual mean pattern of OLR simulated by the two CPSs is shown in Fig. 10b, c, with mean bias and SCC values shown at the top of the panels. Overall, the two CPSs are able to capture the OLR quite well as compared to the observation. The SAS shows higher bias as compared to EMAN, while the SCC values calculated for the two CPSs are quite close to each other. The seasonal mean OLR simulated by the two CPSs for JJAS and DJFM is also depicted (Figs. 11, 12). Overall, the two CPSs are able to capture the OLR quite well as compared to the observation for both seasons. The SAS shows higher bias as compared to EMAN, while the SCC values calculated for the two CPSs are quite close to each other for both JJAS and DJFM. The SAS produces SCC values comparable to those of EMAN on annual and seasonal basis, yet it shows much higher bias as compared to EMAN.

CPSs in GCMs affect large-scale clouds indirectly by regulating the moisture field, because the cloud liquid water path used for determining cloud optical properties was empirically related to the moisture field (e.g., Kiehl et al. 1998; Kim and Kang 2011). Figure 13 shows vertical profiles of the differences in annual and seasonal mean temperature and specific humidity between two CPSs and observations over the global domain. The error in specific humidity (left column, Fig. 13) and in temperature (right column, Fig. 13) for annual and seasonal means is quite similar. The error is typically larger for the SAS from the surface up to 600 hPa, and lower above 500 hPa. On the other hand, the EMAN shows a lower specific humidity bias at all levels compared to that of SAS. Similarly, the temperature bias calculated by the two CPSs over the globe is quite similar between 1000–800 hPa (EMAN shows slightly higher bias as compared to that of SAS). The EMAN-simulated temperature profile shows clearly less bias in the upper layers (700–200 hPa). Hence, both specific humidity and temperature simulated by EMAN show clear improvements over the global domain as compared to the SAS. In particular, the error is almost half in EMAN-simulated specific humidity at lower levels (1000–700 hPa) as compared to SAS. A similar difference was observed in the two fields (not shown), over the tropical region (0–360, 30°S–30°N), which shows the good performance of EMAN as compared to SAS.

Table 1 Comparison of the simulated and observed precipitation statistics for (a) annual, (b) JJAS, and (c) DJFM obtained from TRMM dataset, and limited to tropical belt (0°–360° E, 30°S–30°N). The TRMM annual estimated convective and stratiform components of precipitation over the tropics are 39.82 and 60.18%, respectively

CPS	Mean (mm/day)	Bias (mm/day)	Bias (%)	SCC	Convective fraction in %	Stratiform fraction in %
(a)						
EMAN	1.44	−0.16	−10	0.74	41.86	58.14
SAS	2.55	0.94	58	0.79	70.2	29.8
(b)						
EMAN	1.46	−0.13	−8	0.75	41.59	58.41
SAS	2.54	0.94	59	0.68	69.58	30.42
(c)						
EMAN	1.45	−0.11	−7	0.74	43.56	56.44
SAS	2.53	0.93	58	0.75	69.5	30.50

5 Relative Merits of One CPS Over the Other

The results described above naturally lead to questions as to why one CPS performs better than the other or more specifically, why EMAN performs better than the SAS. The answers to these questions are not straightforward. Several factors, including formulation and assumptions made in these CPSs, can be responsible for producing different results. Moreover, different CPSs may respond in different ways to a given combination of horizontal and vertical resolutions of the model. The question of why a particular scheme performs better than another can be viewed by the way the schemes have been formulated as already briefly discussed in Sect. 2.

The basic difference between the two CPSs (SAS and EMAN) is that the cloud model used in the SAS is of the "entraining plume", while EMAN employed "buoyancy sorting" concept, which is based on the episodic mixing model of Raymond and Blyth (1986), and consonant with important observed properties of cumulus convective clouds (Emanuel 1991). The Emanuel CPS is meant to represent the effects of all moist convection, including shallow, non-precipitating cumulus, while in case of SAS the non-precipitating shallow cumulus scheme is represented by a separate parameterization, which warrants additional errors or uncertainties. The CAPE closure of the SAS is sensitive to the convective instability and as a result SAS produces too little precipitation from large-scale condensation and too much convective precipitation in the tropics (over 70%) when compared to the TRMM observation (40%). However, the precipitation partition in EMAN scheme is quite realistic which is due to the fact that this scheme not only depends on the CAPE but also this scheme is sensitive to the supply of the moisture. Further, the ability of SAS to perform realistic simulations when run in a very high-resolution model is also problematic. Enomoto et al. (2007) discussed the results obtained with different CPSs in the Atmospheric Model for the Earth Simulator (AFES) with fine resolution. They found that for resolutions finer than about T639 the Arakawa–Schubert type schemes behave very unrealistically in that it produces very little convective rain, and the model stratiform parameterization takes over the production of tropical rain. Further, Enomoto et al. (2007) observed a better performance at fine resolution when employing a version of the Emanuel CPS.

6 Summary and Concluding Remarks

Two CPSs (SAS and EMAN) were tested in the SCM framework by specifying the observed horizontal and vertical advection of temperature and specific humidity as a forcing from TOGA-COARE data for different periods, which include both suppressed and active convection regimes and the transition between them. SCM results with SAS and EMAN were compared with observed variables. The EMAN provides a better simulation of temperature and moisture fields as compared to the SAS. Single-column model precipitation is also improved with the EMAN.

The atmospheric component of the SAUDI-KAU model with two CPSs presents altogether a rather satisfactory climatology of rainfall, OLR, temperature and moisture fields. The model, however, still exhibits significant biases in particular in the precipitation field. It is likely that finer tuning of the convection and cloud schemes could produce a reduction in these biases. Note also that a peculiar behavior of the SAUDI-KAU AGCM with SAS was identified, namely a double ITCZ problem during DJFM, which is also evident in OLR, which is not happening in

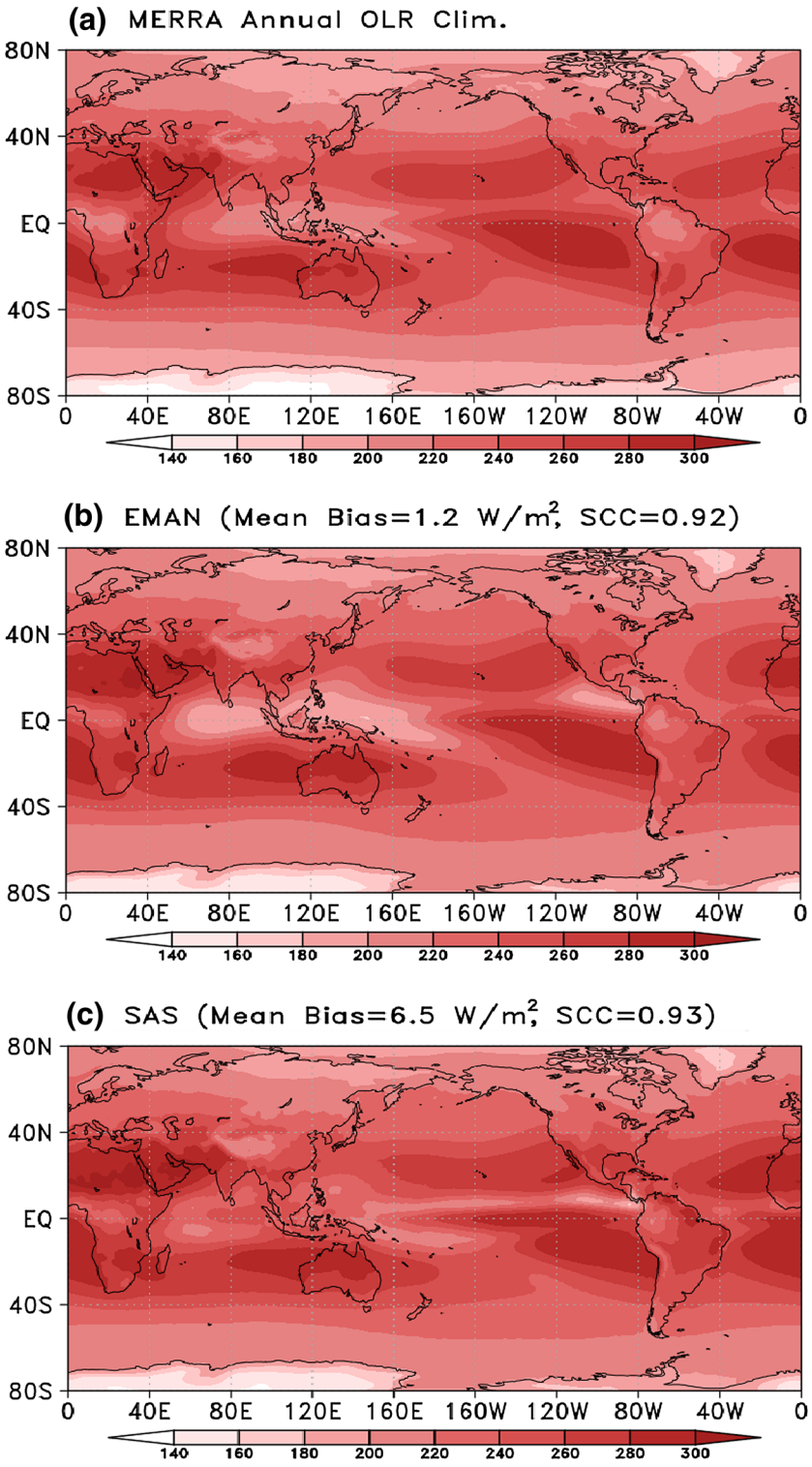

Fig. 10 Same as Fig. 6 but for annual OLR. Unit is W/m^2

case of EMAN. The model also tends to produce too little rainfall over dry regions of the globe including the Arabian Peninsula during DJFM for both SAS and EMAN. Despite those biases, the SAUDI-KAU AGCM current version represents a significant step forward with respect to the base SNU-GCM. We have shown in particular that the

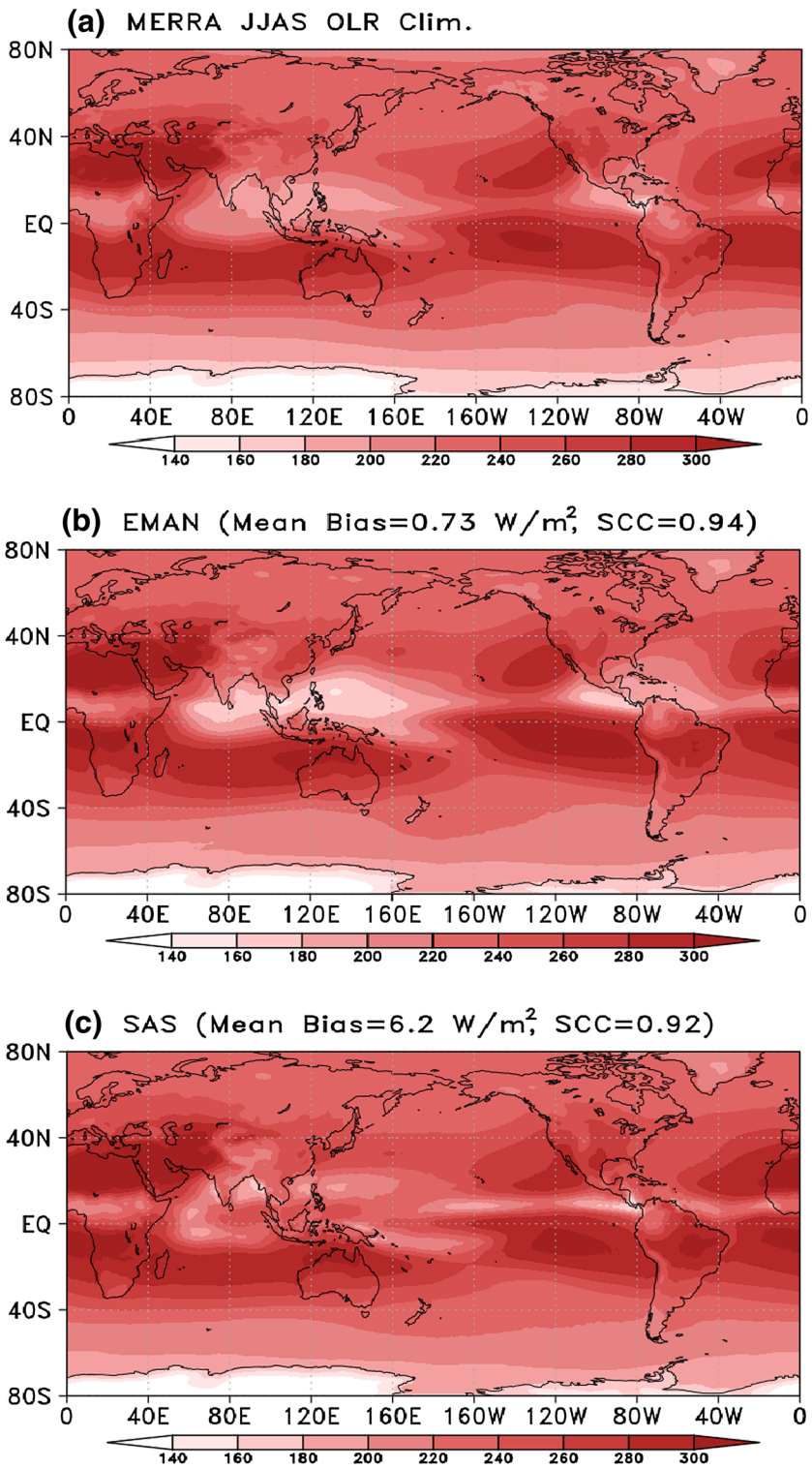

Fig. 11 Same as Fig. 7 but for JJAS OLR. Unit is W/m^2

replacement of the SAS by EMAN has a major and generally positive impact in the tropics. The vertical distributions of temperature and moisture fields are much improved in EMAN simulations as compared to those using in SAS. The coupling of the convection scheme with a PDF-based cloud scheme also has a positive impact on

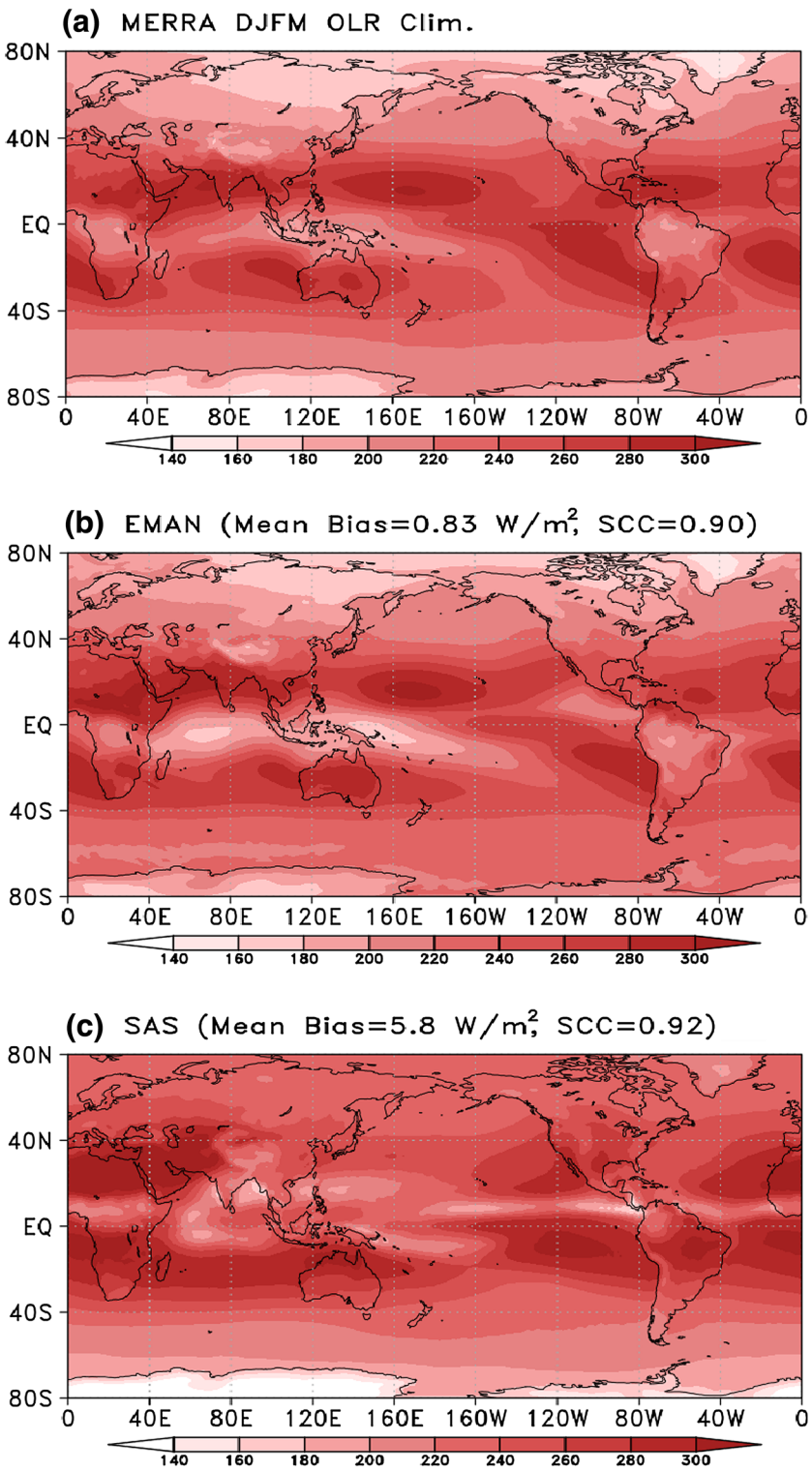

Fig. 12 Same as Fig. 8 but for DJFM OLR. Unit is W/m^2

overall performance of the model, which includes global distribution of OLR comparable to MERRA, and less bias (about 1 W/m^2 in EMAN as compared to SAS which has about 5 W/m^2) in OLR for annual and seasonal simulations. The better performance of the EMAN scheme in reproducing the climatic mean fields may have positive

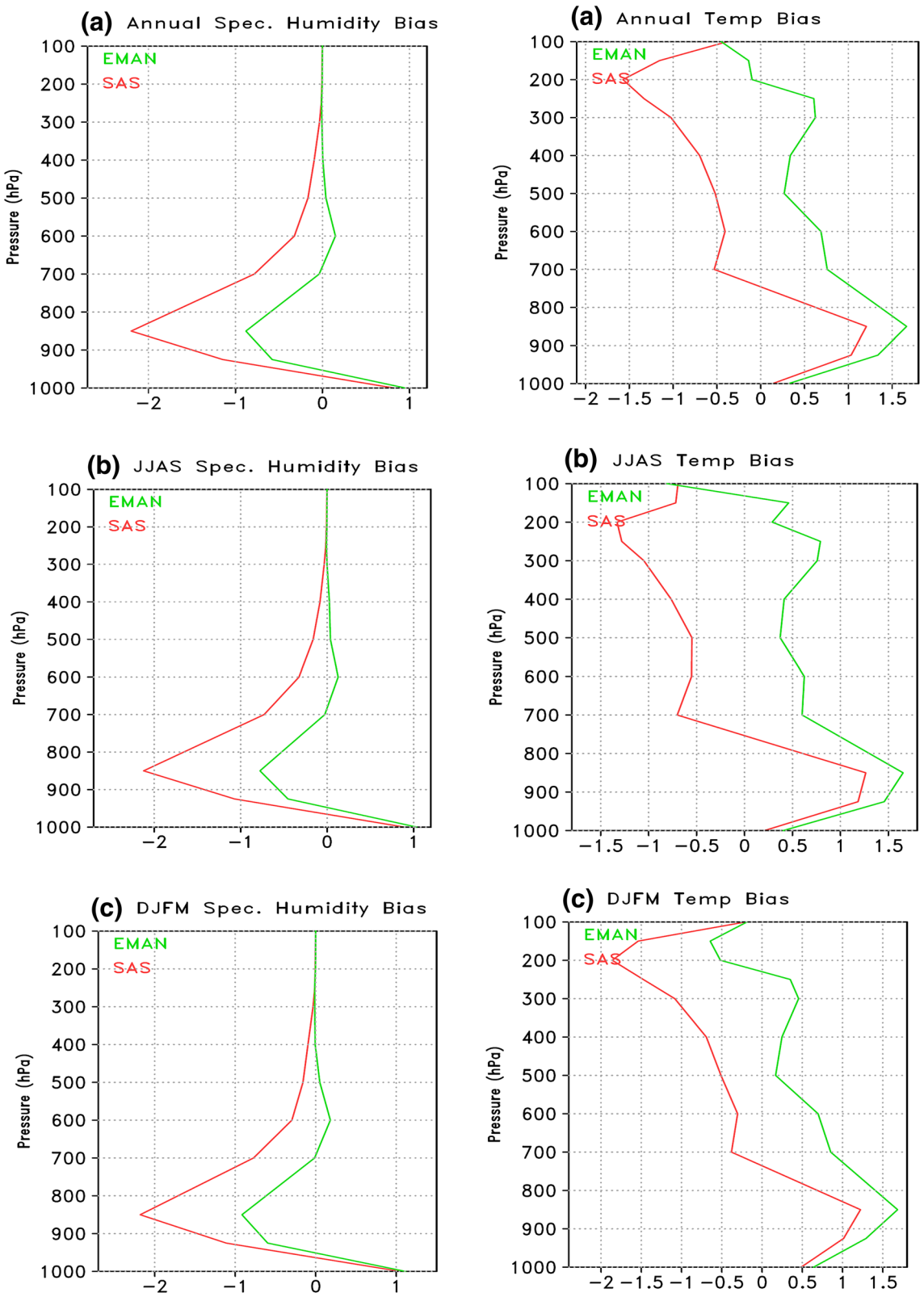

Fig. 13 Bias of (model–observation) JJAS: **a** specific humidity (unit = g/kg) **b** temperature (unit = °C) with two different convection schemes (EMAN and SAS) from 1981 to 2014. The specific humidity and temperature are horizontally averaged over the tropics (0°–360°, 30°S–30°N)

consequences in depicting the seasonal mean variability and predictability and further research is in progress to explore these issues.

Acknowledgements This work represents a part of the first author PhD research work. The authors would like to take this opportunity to thank Prof. Kerry Emanuel at MIT for providing the computer code for the Emanuel scheme. The authors would like to acknowledge the contribution from the anonymous reviewers whose useful comments and suggestion helped us to improve the present research paper. The authors would also like to acknowledge the Center of Excellence for Climate Change Research (CECCR), Department of Meteorology, Deanship of Graduate Studies and Deanship of Scientific Research, King Abdulaziz University (KAU), Jeddah, Saudi Arabia, for providing the necessary support to carry out this study. Computation for the work described in this paper was supported by King Abdulaziz University's High Performance Computing Center (Aziz Supercomputer: http://hpc.kau.edu.sa).

References

Adler RF et al (2003) The version 2 global precipitation climatology project (GPCP) monthly precipitation analysis (1979-present). J Hydrometeorol 4:1147–1167

Arakawa A (2004) The cumulus parameterization problem: past, present, and future. J Clim 17:2493–2525

Arakawa A, Schubert WH (1974) Interaction of a cumulus ensemble with the large-scale environment, part I. J Atmos Sci 31:674–704

Betts AK, Miller MJ (1986) A new convective adjustment scheme. Part II: single column tests using GATE wave, BOMEX, ATEX and arctic air-mass data sets. Q J R Meteorol Soc 112:693–709

Bonan GB (1996) The land surface climatology of the NCAR land surface model coupled to the NCAR Community Climate Model. J Clim 11:1307–1326

Bony S, Emanuel KA (2001) A parameterization of the cloudiness associated with cumulus convection; evaluation using TOGA COARE data. J Atmos Sci 58:3158–3183

Dee DP et al (2011) The ERA-interim reanalysis: configuration and performance of the data assimilation system. Q J R Meteorol Soc 137:553–597

Ehsan MA et al (2017) Sensitivity of AGCM simulated regional summer precipitation to different convective parameterizations. Int J Climatol. doi:10.1002/joc.5108

Emanuel KA (1991) A scheme for representing cumulus convection in large-scale models. J Atmos Sci 48:2313–2335

Emanuel KA, Zivkovic-Rothman M (1999) Development and evaluation of a convection scheme for use in climate models. J Atmos Sci 56:1766–1782

Enomoto T, Kuwano-Yoshida A, Komori N, Ohfuchi W (2007) Description of AFES 2: improvements of high-resolution and coupled simulations. In: Ohfuchi W, Hamilton K (eds) High resolution numerical modelling of the atmosphere and ocean, Chap 5. Springer Publications, Berlin

Gregory D, Rowntree PR (1990) A mass flux convection scheme with representation of cloud ensemble characteristics and stability-dependent closure. Mon Wea Rev 118:1483–1506

Holtslag AAM, Boville BA (1993) Local versus non-local boundary layer diffusion in a global climate model. J Clim 6:1825–1842

Huffman GJ, Adler RF, Bolvin DT, Gu GJ, Nelkin EJ, Bowman KP, Hong Y, Stocker EF, Wolff DB (2007) The TRMM multisatellite precipitation analysis (TMPA): quasi-global, multiyear, combined-sensor precipitation estimates at fine scales. J Hydrometeorol 8:38–55

Kain JS, Fritsch JM (1993) Convective parameterization for mesoscale models: the Kain–Fritsch scheme. The representation of cumulus convection in numerical models of the atmosphere. In: Emanuel KA, Raymond DJ (eds) Meteorology nonographs, No. 46. Amer Meteor Soc, USA, pp 165–170

Kanamitsu M, Ebisuzaki W, Woollen J, Yang SK, Hnilo JJ, Fiorino M, Potter GL (2002) NCEP-DOE AMIP-II reanalysis (R-2) dynamical seasonal forecast system 2000. Bull Am Meteor Soc 83:1631–1643

Kang HS, Hong SY (2008) Sensitivity of the simulated East Asian summer monsoon climatology to four convective parameterization schemes. J Geophys Res 113:D15119. doi:10.1029/2007JD009692

Khairoutdinov M, Randall DA (2001) A cloud resolving model as a cloud parameterization in the NCAR community climate system model: preliminary results. Geophys Res Lett 28:3617–3620

Kiehl JT, Hack JJ, Bonan GB, Boville BB, Williamson DL, Rasch PJ (1998) The National Center for Atmospheric Research Community Climate Model: CCM3. J Clim 11:1131–1150

Kim D, Kang IS (2011) A bulk mass flux convection scheme for a climate model: description and moisture sensitivity. Clim Dyn 38:411–429

Kuo HL (1965) On the formation and intensification of tropical cyclones through latent heat release by cumulus convection. J Atmos Sci 22:40–63

Le Treut H, Li ZX (1991) Sensitivity of an atmospheric general circulation model to prescribed SST changes: feedback effects associated with the simulation of cloud optical properties. Clim Dyn 5:175–187

Lee MI, Kang IS, Kim JK, Mapes BE (2001) Influence of cloud-radiation interaction on simulating tropical intraseasonal oscillation with an atmospheric general circulation model. J Geophys Res 106:14219–14233

Lee MI, Kang IS, Mapes BE (2003) Impacts of cumulus convection parameterization on aqua-planet AGCM simulations of tropical intraseasonal variability. J Meteorol Soc Jpn 81:963–992

Nakajima T, Tsukamoto M, Tsushima Y, Numaguti A (1995) Modelling of the radiative process in an AGCM. In: Matsuno T (ed) Climate system dynamics and modelling, vol I–3, pp 104–123

Numaguti A, Takahashi M, Nakajima T, Sumi A (1995) Development of an atmospheric general circulation model. In: Matsuno T (ed) Climate system dynamics and modelling, vol I–3, pp 1–27

Pezzi LP, Cavacanti IFA, Mendonca AM (2008) A sensitivity study using two different convection schemes over South America. Rev Bras de Meteorol 23:170–190

Randall DA, Xu KM, Somerville RJC, Iacobellis S (1996) Single column models and cloud ensemble models as links between observations and climate models. J Clim 9:1683–1697

Raymond DJ (1995) Regulation of moist convection over the west Pacific warm pool. J Atmos Sci 52:3945–3959

Raymond DJ, Blyth M (1986) A stochastic model for nonprecipitating cumulus clouds. J Atmos Sci 43:2708–2718

Rayner NA, Parker DE, Horton EB, Folland CK, Alexander LV, Rowell DP, Kent EC, Kaplan A (2003) Global analyses of sea surface temperature, sea ice, and night marine air temperature since the late nineteenth century. J Geophys Res 108:4407. doi:10.1029/2002JD002670

Rienecker MM et al (2011) MERRA: NASA's modern-era retrospective analysis for research and applications. J Clim 24:3624–3648

Stan C, Khairoutdinov M, DeMott CA, Krishnamurthy V, Straus DM, Randall DA, Kinter JL III, Shukla J (2010) An ocean–atmosphere climate simulation with an embedded cloud resolving model. Geophys Res Lett 37:L01702. doi:10.1029/2009GL040822

Tiedtke M (1984) The effect of penetrative cumulus convection on the large-scale flow in a general circulation model. Beitrage zur Physik der Atmosphare 57:216–239

Tiedtke M (1989) A comprehensive mass flux scheme for cumulus parameterization in large-scale models. Mon Weather Rev 117:1779–1800

Tost H, Jöckel P, Lelieveld J (2006) Influence of different convection parameterizations in a GCM. Atmos Chem Phys 6:5475–5493

Wang B, Ding Q, Fu X, Kang I-S, Jin K, Shukla J, Doblas-Reyes F (2005) Fundamental challenge in simulation and prediction of summer monsoon rainfall. Geophys Res Lett 32:L15711. doi:10.1029/2005GL022734

Webster PJ, Lukas R (1992) TOGA COARE: the coupled ocean atmosphere response experiment. Bull Am Meteorol Soc 73:1377–1416

Wu R, Kirtman B, Pegion K (2006) Local air–sea relationship in observations and model simulations. J Climate 19:4914–4932

Yang YM, Kang IS, Almazroui M (2014) A mass flux closure function in a GCM based on the Richardson number. Clim Dyn 42:1129–1138

Yousef AE, Ehsan MA, Almazroui M, Assiri ME, Al-Khalaf AK (2017) An improvement in mass flux convective parameterizations and its impact on seasonal simulations using a coupled model. Theor Appl Climatol 127:779–791. doi:10.1007/s00704-015-1668-7

Zhang GJ, McFarlane NA (1995) Sensitivity of climate simulations to the parameterization of cumulus convection in the Canadian climate centre general circulation model. Atmos Ocean 33:407–446

Zhang GJ, Mu M (2005) Effects of modifications to the Zhang-McFarlane convection parameterization on the simulation of the tropical precipitation in the national center for atmospheric research community climate model, version 3. J Geophys Res 110:1–12